Shielding Superconductors with Thin Films as Applied to rf Cavities for Particle Accelerators

Sam Posen,[1,*] Mark K. Transtrum,[2] Gianluigi Catelani,[3] Matthias U. Liepe,[1] and James P. Sethna[4]

[1]*LEPP, Physics Department, Newman Laboratory, Cornell University, Ithaca, New York 14853-2501, USA*

[2]*Department of Physics and Astronomy, Brigham Young University, Provo, Utah 84602, USA*

[3]*Forschungszentrum Jülich, Peter Grünberg Institut (PGI-2), 52425 Jülich, Germany*

[4]*LASSP, Physics Department, Clark Hall, Cornell University, Ithaca, New York 14853-2501, USA*

(Received 29 June 2015; revised manuscript received 27 September 2015; published 29 October 2015)

Determining the optimal arrangement of superconducting layers to withstand large-amplitude ac magnetic fields is important for certain applications such as superconducting radio-frequency cavities. In this paper, we evaluate the shielding potential of the superconducting-film–insulating-film–superconductor (SIS′) structure, a configuration that could provide benefits in screening large ac magnetic fields. After establishing that, for high-frequency magnetic fields, flux penetration must be avoided, the superheating field of the structure is calculated in the London limit both numerically and, for thin films, analytically. For intermediate film thicknesses and realistic material parameters, we also solve numerically the Ginzburg-Landau equations. It is shown that a small enhancement of the superheating field is possible, on the order of a few percent, for the SIS′ structure relative to a bulk superconductor of the film material, if the materials and thicknesses are chosen appropriately.

DOI: 10.1103/PhysRevApplied.4.044019

I. INTRODUCTION

Can one engineer a better superconducting magnetic shield? How can one optimally arrange materials to maintain complete flux exclusion from a region, and what is the maximum external field that can be screened? It has long been known that superconducting films of width d smaller than the London magnetic penetration depth λ can remain superconducting at much higher magnetic fields than bulk samples [1], so it has been proposed that films could be used to shield bulk superconductors [2]. In this paper, we investigate the shielding properties of the film-insulator-bulk (SIS′) structure and compare to the single superconducting slab. The focus here is on ac rather than dc shielding; the latter has already been studied extensively [3–7].

Superconducting radio-frequency (SRF) cavities are an example of an application in which shielding of large-amplitude high-frequency magnetic fields is required. This technology underlies particle accelerators used in high-energy physics, nuclear physics, neutron sources, and x-ray light sources. The large ac accelerating electric field of these cavities induces a correspondingly large magnetic field. If the magnetic field exceeds the flux penetration field of the material, it causes a quench in the cavity. If SIS′ structures could enhance the flux penetration field relative to that of a bulk superconductor, it could allow these cavities to achieve higher accelerating fields [8]. This has motivated significant experimental effort to fabricate such structures [9–11], although their ability to screen large-amplitude rf magnetic fields has not yet been measured.

In this paper, we examine the superheating fields B_{sh} of these structures, where flux penetration would occur in defect-free superconductors; below B_{sh}, the whole structure can remain in the vortex-free (metastable) Meissner state. In fact, part of the motivation for this work is that there has been significant confusion in the SRF community regarding the maximum fields that SIS′ structures can screen; we hope that this study clarifies the screening mechanism and its limitations. Our calculations show modest shielding gains for SIS′ heterolaminates compared to bulk superconductors. The SIS′ structure may provide benefits in other ways for realistic materials with surface defects [12], but considering those benefits is beyond the scope of the present work.

The paper is organized as follows: We start our analysis by arguing in Sec. II that, for a SIS′ structure, a significant enhancement of the flux penetration field could be achieved only if a significant gradient in the phase of the order parameter $\nabla\phi$ can be established across the film shielding the bulk. Since this would result in a level of dissipation that is likely unmanageable, we restrict our analysis to fields below B_{sh}, where both the film and bulk

*Present address: Fermi National Accelerator Laboratory, Batavia, IL 60510, USA.

superconductor are in the (meta)stable Meissner state, with no phase gradient across the film. In Sec. III, numerical calculations are performed in the London limit. The thin-film regime is examined in Sec. IV with an analytical Ginzburg-Landau approach. In Sec. V, the results are extended to films of intermediate thicknesses via a full numerical Ginzburg-Landau analysis. We summarize our work in Sec. VI.

II. FLUX EXCLUSION

The fundamental link between superconducting order and magnetism is the fact that the free energy and properties of the system are governed not by the gradients $\nabla\psi$ of the superconducting order parameter but by a "covariant" derivative $D\psi = (\nabla - e^*\mathrm{i}\mathbf{A}/\hbar)\psi$, where $e^* = 2e$ is the Cooper pair charge and $\mathbf{A}$ is the magnetic vector potential [1]. If we write the complex order parameter in terms of two real functions as $\psi = |\psi|\exp(\mathrm{i}\phi)$, the covariant derivative becomes

$$D\psi = [\nabla|\psi| + \mathrm{i}|\psi|(\nabla\phi - e^*\mathbf{A}/\hbar)]\exp(\mathrm{i}\phi) \quad (1)$$

$$= [\nabla|\psi| + \mathrm{i}|\psi|(m^*\mathbf{v}_s/\hbar)]\exp(\mathrm{i}\phi), \quad (2)$$

where the gauge-invariant combination

$$(\hbar/m^*)(\nabla\phi - e^*\mathbf{A}/\hbar) = \mathbf{v}_s \quad (3)$$

is called the *supercurrent velocity*. Magnetic fields cause "stress" in superconductors indirectly through $\mathbf{A}$, which induces screening supercurrents. Because of these supercurrents, a weak magnetic field exponentially decays inside a superconductor over the penetration depth λ. As a crude approximation, the superconductor can support a certain maximum stress, characterized by a maximum supercurrent velocity $\mathbf{v}_s^{\max}$. The superconductor can screen A values larger than $v_s^{\max}m^*/e^*$ only if it passes vortex lines through its boundary. For example, if a vortex line is passed through a hollow superconducting cylinder in a parallel external field, this will bring flux inside the cylinder and ϕ will wind by a factor of 2π, lowering the stress in the superconductor.

Now let us consider a single thin superconducting film separated from a bulk superconductor by a thin insulator, shown in Fig. 1. In a "thin" superconductor of thickness $d \ll \lambda$, the critical fields are enhanced; for example, for the parallel thermodynamic critical field, we have $H_{c\|} = 2\sqrt{6}(H_c\lambda/d)$ [1]. The Meissner state requires $\mathbf{A} \to 0$ deep in the bulk, and $\mathbf{A}$ is continuous across the insulating gap. Therefore, the vector potential at the film surface is tied to that of the bulk superconductor surface; however, the insulating gap offers the opportunity to decouple the phase gradient across the film from that in the bulk. If many vortex lines pass through the film, the superconducting film could be relatively unstressed, supplementing the native superheating field of the film material.

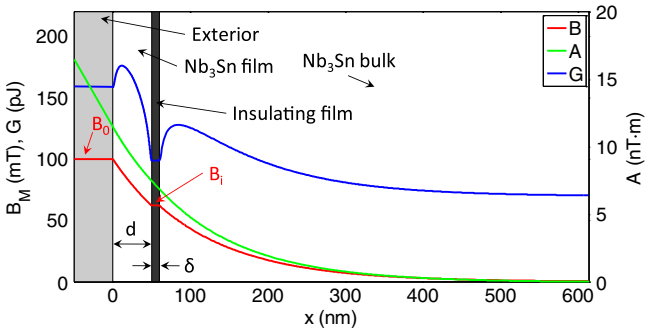

FIG. 1. Example of a SIS′ structure. The amplitudes of the magnetic field, the vector potential, and the Gibbs free energy are plotted as a function of distance into the structure.

In the dc limit, it should be possible to screen a bulk from very large fields by using a compound film with many layers of alternating thin superconducting and insulating films with magnetic flux trapped between each of them. However, in ac applications, filling the insulators with magnetic flux demands the transfer of $\nabla\phi/\pi$ fluxoids per unit length across the screening film in each cycle. The ac response of a superconductor with vortices has been considered before—see, e.g., Refs. [13–15]. Here we simply note that, as they pass through the film, the vortices would experience strongly dissipative drag [2], generating levels of heating that are likely unmanageable for most applications [16].

As we are focusing on rf applications, we impose the restriction that flux must never pass into the superconducting regions. With this restriction, the SIS′ structure would offer an advantage over a single thick superconducting slab if it could withstand higher magnetic fields without flux penetration. Since the frequencies we are interested in are much smaller than the gap, the superconducting order parameter depends only on the instantaneous value of the magnetic field. The flux-free state is intrinsically stable only below B_{c1}, the lower critical field. However, there is good evidence that real materials can withstand rf fields well above B_{c1} [17,18]. As the field is pushed above B_{c1} and then again below it, the superconductor does not have time to relax to its equilibrium (mixed) state but is rather in a metastable Meissner state. In this metastable regime, an energy barrier prevents flux from penetrating, a barrier that is reduced to zero at B_{sh} for a defect-free material (thermal fluctuations at cryogenic temperatures are much smaller than the condensation energy, so they cannot create excitations above the barrier). B_{sh} is the ultimate ac magnetic limit; this is especially important for SIS′ films, as they are always in the metastable state [16]. We use $B_{\mathrm{sh}}^{\mathrm{SIS}'}$ to denote the maximum metastable field of a SIS′ structure to distinguish it from the superheating field of the bulk material, $B_{\mathrm{sh},b}$, and the bulk superheating field of the film material, $B_{\mathrm{sh},f}$ (i.e., the value it would have if it were not a thin film). In the next three sections, we present and

compare three approaches to calculate $B_{\rm sh}^{\rm SIS'}$. We study this limit quantitatively, to evaluate how useful these structures would be for real applications. We show that the SIS′ structure leads to a small increase in the maximum field, much smaller than the manifold increase in the parallel critical field of thin films mentioned above and that motivated the proposal in Ref. [2].

III. SUPERHEATING FIELD IN THE LONDON LIMIT

To make a rough estimate of the superheating field of the SIS′ structure, we consider the Gibbs free energy $\mathcal{G}$ in the London limit; that is, we assume that both film and bulk superconductors are strongly type-II materials, with penetration depths much longer than coherence lengths. We denote by λ_f the film's material penetration depth and by ξ_f its coherence length. The thickness d of the film is assumed to be much larger than ξ_f; in particular, for the vortex core to be accommodated in the film, one needs $d \gtrsim 1.8\xi_f$ [19,20]. The film is separated from a bulk superconductor with penetration depth λ_b by an insulating film of thickness δ. The superconducting film is screening the bulk from a parallel magnetic field with amplitude B_0. The screened field between the film and the bulk has amplitude B_i. In our geometry, the x axis is perpendicular to the film, pointing into it, with the origin at the interface with the exterior. The z axis is aligned with the magnetic field.

The Gibbs free energy of a vortex in a superconductor can be determined from the value of two magnetic fields evaluated at the vortex location r_0, the Meissner-screened external field B_M and the field generated by the vortex in the film B_V [21]:

$$\mathcal{G} = \frac{\phi_0}{\mu_0}[B_V(r_0)/2 + B_M(r_0)], \tag{4}$$

where ϕ_0 is the flux quantum and μ_0 the magnetic constant. The field B_M can be found by minimizing the free energy in the structure when no vortex is present; we recall that in the London limit the Meissner field in the bulk superconductor decays exponentially, and hence it equals $B_i e^{-[x-(d+\delta)]/\lambda_b}$. This procedure gives

$$B_M = \frac{B_0 + B_i}{2}\frac{\cosh\frac{x-d/2}{\lambda_f}}{\cosh\frac{d}{2\lambda_f}} - \frac{B_0 - B_i}{2}\frac{\sinh\frac{x-d/2}{\lambda_f}}{\sinh\frac{d}{2\lambda_f}}, \tag{5}$$

where B_i is given by

$$B_i = B_0\left[\frac{\delta+\lambda_b}{\lambda_f}\sinh\frac{d}{\lambda_f} + \cosh\frac{d}{\lambda_f}\right]^{-1}. \tag{6}$$

Explicit formulas for B_V are available for thin ($d \ll \lambda_f$) and thick ($d \gg \lambda_f$) films [21]. To study the full range of thicknesses, we use the more general expression of Ref. [22] [this expression assumes $r_0 = (x_0, 0)$]:

$$B_V = \frac{2\phi_0}{\lambda^2 d}\sum_{n=1}^{\infty}\int_{-\infty}^{\infty}\frac{dk}{2\pi}e^{iky}\frac{\sin(\pi n x/d)\sin(\pi n x_0/d)}{k^2 + (\pi n/d)^2 + 1/\lambda^2}. \tag{7}$$

Equations (5)–(7) give the fields in the structure, and Eq. (4) gives the Gibbs free energy as shown in Fig. 1. The barrier to flux penetration is due to the positive slope of $\mathcal{G}$ inside the superconducting regions near the interfaces. We can find $B_{\rm sh}^{\rm SIS'}$ by finding the field at which the barrier is reduced to zero in any of the superconductors [23]. In Fig. 2, $B_{\rm sh}^{\rm SIS'}$ is plotted as a function of the superconducting film thickness for various SIS′ structures. Various insulator thicknesses are considered, including the thin layer limit, for illustrative purposes as it gives the highest fields. The materials analyzed are those that are promising for SRF cavities, with properties given in Table I.

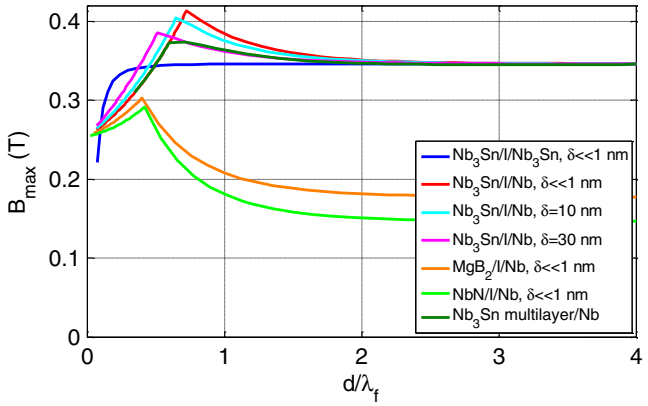

FIG. 2. Maximum field below $B_{\rm sh}$ of both the film and the bulk as a function of film thickness for various film materials in a SIS structure with Nb. The effect of varying the insulator thickness δ is shown for the Nb_3Sn film, as is the effect of splitting the film thickness d over five equally thick multilayers with thin separating insulators. All calculations are done in the London limit.

The structures plotted in Fig. 2 can be divided into two types: homolaminates, in which the film is the same material as the bulk, and heterolaminates, in which they are different. Calculations show that for a homolaminate like Nb_3Sn-insulator-Nb_3Sn, the film is the weak point: It always reaches its $B_{\rm sh}$ before the bulk, and the thinner the film, the lower its $B_{\rm sh}$. Homolaminates with films that are so thick that they behave like a bulk superconductor have the highest $B_{\rm sh}^{\rm SIS'}$. To better understand this, consider the magnetic forces on a vortex [which can be derived from Eq. (4)]. The boundary condition imposed by B_V can be satisfied by an image antivortex outside of the boundary, which creates a force that pulls the vortex out of the film [32]. As the film thickness is reduced, B_M remains approximately unchanged, but the image antivortex on the insulator side of the film used to satisfy B_V has a

TABLE I. Materials parameters of niobium and three promising alternative SRF materials. The penetration depth λ is calculated by using Eq. (3.131) in Ref. [1]. The correlation length ξ is calculated by using the equations in Ref. [24]. For Nb, a residual resistivity ratio of 100 is assumed. For MgB_2, λ and ξ are not calculated, as the experimental values are given in the reference. For calculations, $B_c = \phi_0/(2\sqrt{2}\pi\xi\lambda)$ is used [1]. B_{c1} for Nb found from a power-law fit to numerically computed data from Refs. [25,26] and for strongly type-II materials is found from Eq. (5.18) in Ref. [1]. B_{sh} is calculated by using $B_{sh} \simeq B_c[(\sqrt{20}/6) + (0.5448/\sqrt{\kappa})]$ from Ref. [27]. Nb data are from Ref. [28], Nb_3Sn data from Ref. [29], NbN data from Ref. [30], and MgB_2 data from Ref. [31]. Note that the two-gap nature of MgB_2 may require more careful analysis than is performed here.

Material	λ (nm)	ξ (nm)	B_{c1} (T)	B_c (T)	B_{sh} (T)
Nb	40	27	0.13	0.21	0.25
Nb_3Sn	111	4.2	0.042	0.50	0.42
NbN	375	2.9	0.006	0.21	0.17
MgB_2	185	4.9	0.017	0.26	0.21

stronger effect, as shown in Fig. 3. This lowers the barrier to penetration.

The differing penetration depths in the layers of a heterolaminate cause it to behave differently than a homolaminate. Here we consider structures in which the bulk has a smaller penetration depth than the film. For such structures, if the film is very thin, it does not provide much screening for the bulk, and B_i reaches the bulk's B_{sh} before the thin-film barrier disappears. As with a homolaminate, a very thick film behaves like a bulk and reaches that material's bulk B_{sh} while B_i is still relatively small. However, between these two extremes, there is a situation in which the film provides some screening, so that B_i is large but still smaller than B_0. In this case, a benefit can be realized—the small penetration depth of the material in the bulk causes B_i to be larger than with the exponential decay expected for a thick film [Eq. (6)]. This in turn reduces the magnitude of the negative gradient in B_M, bolstering the barrier to flux penetration [Eq. (4)]. This increase in the barrier is depicted in Fig. 4. The dark curves show B_M, B_V, and $\mathcal{G}$ for a Nb_3Sn thin-film–insulator–Nb bulk SIS structure with a 10-nm-thick insulator and $d/\lambda_f = 0.64$

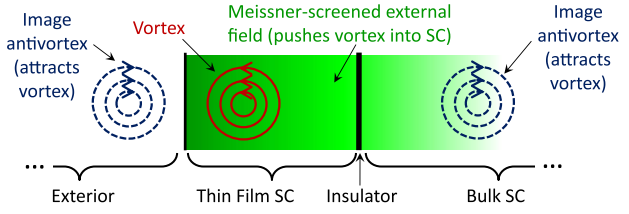

FIG. 3. Forces on a vortex in a homolaminate. As the film is made thinner, the image antivortex to the right of the film has a stronger pull on the vortex, lowering the barrier to vortex penetration.

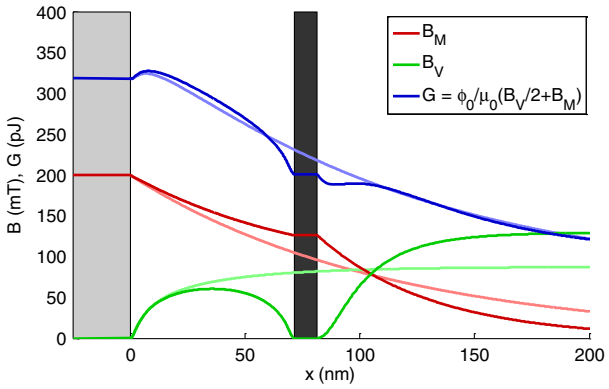

FIG. 4. Comparison of a SIS′ film with near-optimal parameters (dark curves) to a bulk film (light curves). The slower decay of B_M in the large-λ thin film influences $\mathcal{G}$, bolstering the barrier to flux penetration. Note that the dark shaded region representing the insulating region of the SIS′ can be ignored for the bulk film.

(the peak of the cyan curve in Fig. 2). The light curves show calculations for a bulk Nb_3Sn film (for this case, the dark shaded region representing the insulator does not apply). In this example, $B_0 = 300$ mT. The Gibbs free energy of the SIS′ structure is still sharply peaked, showing a relatively robust energy barrier, but that of the bulk film is almost flat, showing that flux penetration is likely to occur at slightly higher fields.

The impact of this is a modest increase in $B_{sh}^{SIS'}$ for these structures compared to the bulk value of the film material. However, the range of film thicknesses over which the increase is appreciable ($\gtrsim$ a few percent) is relatively small, and the gain decreases as the thickness of the insulating layer increases.

IV. THIN FILMS IN THE GINZBURG-LANDAU APPROACH

Calculating B_{sh} using the London theory, as done in the previous section, fails to take into account 2D instabilities in the order parameter, therefore overestimating B_{sh} in many circumstances. The problem of calculating B_{sh} for bulk samples while taking into account 2D instabilities has a long history (see, e.g., Ref. [27]) and has mostly been tackled in the Ginzburg-Landau (GL) framework. Only recently were calculations beyond the GL theory performed [33,34]; they show that, while the GL results cannot be trusted quantitatively at low temperatures, they give a qualitatively correct estimate. Therefore, for simplicity, we restrict ourselves to the GL theory even in the low-temperature regime where its quantitative predictions are not exact.

The approach we use to find B_{sh} is described in detail in Ref. [27]: We first extremize the GL free energy, a functional of the spatially dependent order parameter ψ and supercurrent velocity $\mathbf{v}_s$, and then study its stability against small perturbation of these functions. In the present case,

the GL free energy is the sum of the contributions for the bulk and the film. The boundary conditions are the usual ones for the order parameter (vanishing of its derivatives at all surfaces); the supercurrent velocity vanishes deep into the bulk, and its derivative at the external film surface is proportional to the applied magnetic field. Similarly, the field between the film and the bulk is proportional to the derivatives of the supercurrent velocities at the two surfaces. However, this internal field is not externally imposed but must be calculated consistently with Maxwell equations; this gives the final condition of continuity of the vector potential across all surfaces. Hence, for a very thin insulating barrier, the supercurrent velocities at the bulk surface and the internal film surface coincide, while the film supercurrent velocity would be higher for a thicker insulator.

For an analytical estimate of the SIS′ superheating field $B_{\rm sh}^{\rm SIS'}$, we consider the simplest possible case of a strongly type-II bulk material (GL parameter $\kappa_{\rm GL} \gg 1$) shielded by an insulator of negligible thickness and a strongly type-II thin film with $\xi_f \ll d \ll \lambda_f$. With a thin film, the difference between the internal field (at the bulk surface) and the applied field (outside the film) is small, and the maximum possible field is reached when the internal field coincides with the bulk superheating field $B_{{\rm sh},b}$. Indeed, within the GL theory and at linear order in d/λ_f, using the boundary conditions discussed above we find [see the Appendix]

$$B_{\rm sh}^{\rm SIS'} = B_{{\rm sh},b}\left[1 + \sqrt{\frac{6}{5}}\frac{\lambda_b}{\lambda_f}\left(1 - \frac{v_{s,r}^2}{3}\right)\frac{d}{\lambda_f} + \frac{1}{2}(1 - v_{s,r}^2)\left(\frac{d}{\lambda_f}\right)^2\right], \tag{8}$$

where $v_{s,r} = v_{s,b}^{\rm max}/v_{s,f}^{\rm max}$ is the ratio of the maximum supercurrent velocities for the bulk and film material, respectively. This ratio can be written in terms of critical fields and penetration depths as $v_{s,r} = B_{c,b}\lambda_b/B_{c,f}\lambda_f$, and as a necessary condition for metastability it must satisfy $v_{s,r} < 1$: Since in the bulk material the supercurrent velocity has already reached its maximum possible value at the surface, the film material must be able to support a higher supercurrent velocity. We stress again that, for sufficiently thin films (below the critical thickness discussed in the next paragraph), as the applied field becomes larger than $B_{\rm sh}^{\rm SIS'}$, the bulk becomes unstable, while the film is still (meta)stable. As qualitatively expected, Eq. (8) shows that for better screening a thicker film should be used and that, as the film material penetration depth increases, its screening power decreases. Also, the need of small v_s^r implies that the film material critical field should be sufficiently large: $B_{c,f} > B_{c,b}\lambda_b/\lambda_f$. Interestingly, based on the values reported in Table I, this condition can be met if using Nb_3Sn or MgB_2 to shield Nb.

We note, however, that there is in principle a limit on how thick the film can be made: Since the supercurrent velocity at the film external surface increases with thickness, if the film is too thick, it will become unstable at a field below that predicted by Eq. (8). Within our approximations, we find that the critical thickness for the film to also become unstable at $B_{\rm sh}^{\rm SIS'}$ is $d_c = \lambda_f\sqrt{6/5}(1 - v_{s,r})B_{c,f}/B_{c,b}$. We see that the condition $d < d_c$ can severely restrict the maximum film thickness only in the regime $B_{c,f} \ll B_{c,b}$, $\lambda_f \gg \lambda_b$. For the material parameters in Table I, our formula gives $d_c \sim \lambda_f$, but films of this thickness are beyond the approximate analytical treatment that leads to Eq. (8). Therefore, to study the screening properties of films of intermediate thickness, $d \sim \lambda_f$, in the next section we resort to numerical calculations that also account for the finite value of $\kappa_{\rm GL}$.

V. FILMS OF INTERMEDIATE THICKNESS

For films of intermediate thickness, numerical techniques are needed to accurately estimate the effective superheating field of SIS structure in the Ginzburg-Landau theory. Here, we follow closely the methods described in Ref. [27]. It is shown there that, in the bulk, three quantities characterize the system: coherence length ξ, penetration depth λ, and thermodynamic critical field B_c, which we give in Table I for some materials of interest.

The Ginzburg-Landau equations are solved in each domain separately, and then boundary conditions are matched. In order to improve numerical stability, we implement the boundary conditions as follows: At the film surface, the gradient of the order parameter is fixed to zero while the magnitude is allowed to vary, effectively defining the applied magnetic field implicitly in terms of the order parameter. We also allow the value of the order parameter and the vector potential on the film side of the interface to vary. On the bulk side of the interface, the gradient of the magnetic field is fixed to zero while its magnitude is allowed to vary. Infinitely deep in the bulk, the order parameter is fixed to one and the vector potential vanishes. This configuration introduces three parameters for the boundary conditions: the magnitude of the order parameter on either side of the interface and the magnitude of the vector potential on the film side of the interface. These three parameters are varied, until the gradient of the order parameter vanishes on the film side of the interface and both the magnetic vector potential and the magnetic field are continuous at the interface.

Having found a solution, we next solve the eigenvalue problem associated with the stability of the solution to infinitesimal fluctuations of wave number k as in Ref. [27]. These solutions are also found numerically by using boundary conditions similar to those just described. The magnitude of the applied magnetic field and the

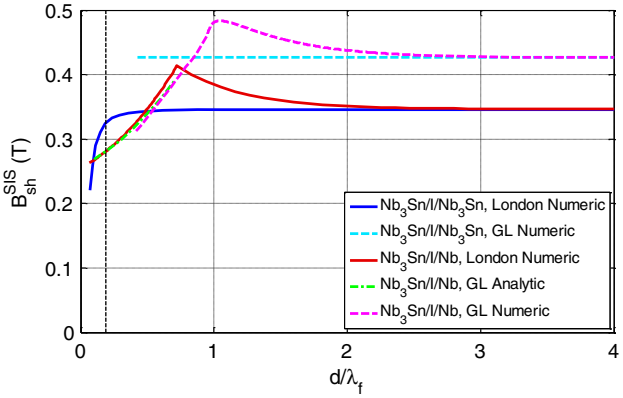

FIG. 5. B_{sh} in a SIS′ structure as a function of film thickness. The insulating layer is assumed to be very thin. London-limit calculations are compared to Ginzburg-Landau analytical and numerical calculations. For reference, the dashed vertical line is at the position $d \sim 5\xi_f \sim \sqrt{\lambda_f \xi_f}$. We recall that the results of Secs. III (solid lines) and IV (dot-dashed line) are valid for films thick compared to ξ_f. Calculations and simulations are done by using material parameters from Table I.

wave number are then varied simultaneously to identify the least-stable fluctuation and the applied magnetic field at which it just becomes unstable (i.e., at which the eigenvalue becomes zero). In this way, we identify the superheating field and the critical wave number that characterizes the unstable fluctuations. These calculations are summarized in Fig. 5, in which we plot $B_{sh}^{SIS'}$ as a function of film thickness for various materials. Note that the dashed lines start from thicknesses of about 50 nm. For films with thickness less than this, numerical results become increasingly difficult, presumably due to the extremely separated length scales involved. Interestingly, this thickness coincides with approximately twice the depth $\sqrt{\lambda_f \xi_f}$ of the fluctuations [27], suggesting that interactions between the fluctuations of both film surfaces may become relevant. Moreover, numerical solutions indicate that, at finite κ, the nature of the instability itself may change from 2D to 1D as the thickness decreases. Although beyond the scope of the present work, these indications deserve further investigation.

The Ginzburg-Landau calculations show good qualitative agreement with the London calculations from Fig. 2, also shown in this figure. There are some quantitative differences, likely due to the approximations used in the London limit. For instance, the difference in the calculated bulk B_{sh} of the film material, which is approached as the film becomes a few λ_f thick, is due to the finiteness of κ. For the heterolaminate, in both cases as the film thickness increases, $B_{sh}^{SIS'}$ shows a peak near $d \sim \lambda_f$ and then decreases to the superheating field of the film material as the film becomes very thick. The thickness at which the peak occurs is somewhat smaller for the London limit, but the two plots are otherwise very similar in shape.

VI. CONCLUSIONS

In this study, we analyze the magnetic shielding properties of superconductors at high fields and high frequencies. To prevent strong vortex dissipation due to drag, the analysis is restricted to a regime where flux penetration is not allowed. The London-limit numerical results are verified against analytical and numerical Ginzburg-Landau calculations. We show that the SIS′ structure can produce a modest enhancement of the maximum screening field compared to a single superconducting slab for certain materials and film thicknesses; see the maxima in Fig. 5.

ACKNOWLEDGMENTS

This work is supported by DOE Awards No. DE-SC0002329 and No. DE-SC0008431, NSF Award No. DMR 1312160, and in part the EU under REA Grant Agreement No. CIG-618258.

APPENDIX: DERIVATION OF EQ. (8)

In the case of large GL parameter $\kappa_{GL} \gg 1$, the calculation of the metastability field, Eq. (8), is greatly simplified: For $\kappa_{GL} \to \infty$, the spatial profile of the order parameter is fully determined by that of the supercurrent velocity, and the differential equation for the latter is local, albeit nonlinear [27]. Indicating with q_0 the dimensionless supercurrent velocity, for the geometry we are considering it obeys the equation

$$q_0'' = q_0 - q_0^3, \tag{A1}$$

and the metastability condition takes the simple form $q_0^2 < 1/3$ [27]. The dimensionful velocity is proportional to q_0 multiplied by the critical field and the penetration depth, $v_s \propto B_c \lambda$, and we do not need the proportionality constant in what follows.

For simplicity, in this Appendix we use a coordinate system in which x axis perpendicular to the film has its origin in the middle of the film and measure lengths in units of the film material penetration depth λ_f. We also take the insulator thickness to be negligible, $\delta = 0$, as this gives the highest possible metastable field. As discussed in Secs. III and IV, the instability happens at the bulk surface; this fixes the values of the supercurrent velocity at the interior surface of the film to be

$$q_0\left(\frac{d}{2\lambda_f}\right) = -\sqrt{\frac{1}{3}} v_{s,r}, \qquad v_{s,r} = \frac{B_{c,b}\lambda_b}{B_{c,f}\lambda_f}. \tag{A2}$$

Clearly, a necessary condition for the metastability of the film is $v_{s,r} < 1$. In fact, since the supercurrent velocity at the outer surface is larger, we will further need to check that $q_0^2(-d/2\lambda_f) < 1/3$. In addition to the above boundary condition, we also need the field between the film and bulk to coincide with the bulk superheating field:

$$q_0'\left(\frac{d}{2\lambda_f}\right) = \frac{B_{\mathrm{sh},b}}{\sqrt{2}B_{c,f}}. \tag{A3}$$

The task is now to find the external field at which these two boundary conditions are satisfied:

$$B_{\mathrm{sh}}^{\mathrm{SIS}'} = \sqrt{2}B_{c,f}q_0'\left(-\frac{d}{2\lambda_f}\right). \tag{A4}$$

To solve Eq. (A1), thanks to the assumption $d \ll \lambda_f$, we can proceed by a Taylor expansion of the function $q_0(x)$ near $x = 0$:

$$q_0(x) = q_c + b_0 x + b_1\frac{x^2}{2} + b_2\frac{x^3}{3} + \cdots. \tag{A5}$$

Substituting the expansion into Eq. (A1) and matching the terms on the two sides of the equality, we find

$$b_1 = q_c(1-q_c^2), \qquad b_2 = \frac{1}{2}b_0(1-3q_c^2), \tag{A6}$$

showing that only two parameters of the expansion, q_c and b_0, are left undetermined and thus can be fixed by the boundary conditions. Moreover, Eq. (A4) can be written in the form

$$B_{\mathrm{sh}}^{\mathrm{SIS}'} = B_{\mathrm{sh},b} - \sqrt{2}B_{c,f}q_c(1-q_c^2)\frac{d}{\lambda_f} + \mathcal{O}\left(\frac{d}{\lambda_f}\right)^3, \tag{A7}$$

and hence to calculate $B_{\mathrm{sh}}^{\mathrm{SIS}'}$ to second order in d/λ_f we need only to know q_c to first order. We can therefore use the boundary condition (A3) at lowest order to obtain $b_0 = B_{\mathrm{sh},b}/\sqrt{2}B_{c,f}$ and the boundary condition (A2) at first order to find

$$q_c = -\sqrt{\frac{1}{3}}v_{s,r} - \frac{B_{\mathrm{sh},b}}{\sqrt{2}B_{c,f}}\frac{d}{2\lambda_f}. \tag{A8}$$

Substituting this expression into Eq. (A7) and keeping only terms up to second order, we find

$$B_{\mathrm{sh}}^{\mathrm{SIS}'} = B_{\mathrm{sh},b}\left[1 + \frac{1}{2}(1-v_{s,r}^2)\left(\frac{d}{\lambda_f}\right)^2\right] + \sqrt{2}B_{c,f}\sqrt{\frac{1}{3}}v_{s,r}\left(1-\frac{v_{s,r}^2}{3}\right)\frac{d}{\lambda_f}. \tag{A9}$$

To put this equation in the form given in Eq. (8), we use the relationship [27] $B_{\mathrm{sh},b} = \sqrt{5}B_{c,b}/3$ between superheating and critical fields. Finally, by considering at linear order in d/λ_f the metastability requirement $q_0(-d/2\lambda_f) > -1/\sqrt{3}$, we obtain the critical thickness d_c reported at the end of Sec. IV.

[1] Michael Tinkham, *Introduction to Superconductivity* (Dover, New York, 2004), p. 454.
[2] A. Gurevich, Enhancement of rf breakdown field of superconductors by multilayer coating, Appl. Phys. Lett. **88**, 012511 (2006).
[3] Franco Pavese, in *Handbook of Applied Superconductivity*, edited by Bernd Seeber (Taylor & Francis, London, 1998), Vol. 2, pp. 1461–1483.
[4] S. Denis, Ph.D. thesis, University of Liège, 2007.
[5] J. R. Claycomb and Jr. J. H. Miller, Superconducting magnetic shields for squid applications, Rev. Sci. Instrum. **70**, 4562 (1999).
[6] Y. Obi, M. Ikebe, and H. Fujishiro, Repulsive flux pinning force in NbTi/Nb superconductor/superconductor multilayers, J. Low Temp. Phys. **137**, 125 (2004).
[7] V. Plecháček, E. Pollert, and J. Hejtmánek, Influence of the micro structure on magnetic-shielding properties of (Bi,Pb)-Sr-Ca-Cu-O superconductor, Mater. Chem. Phys. **43**, 95 (1996).
[8] By flux penetration field, we mean the maximum value of the magnetic field just outside the film such that no flux enters into the bulk.
[9] C. Z. Antoine, J.-C. Villegier, and G. Martinet, Study of nanometric superconducting multilayers for RF field screening applications, Appl. Phys. Lett. **102**, 102603 (2013).
[10] Teng Tan, M. a. Wolak, Narendra Acharya, Alex Krick, Andrew C. Lang, Jennifer Sloppy, Mitra L. Taheri, L. Civale, Ke Chen, and X. X. Xi, Enhancement of lower critical field by reducing the thickness of epitaxial and polycrystalline MgB2 thin films, APL Mater. **3**, 041101 (2015).
[11] A.-M. Valente-Feliciano, J. K. Spradlin, G. Eremeev, C. E. Reece, M. C. Burton, and R. A. Lukaszew, in Proceedings of the Seventeenth International Conference on rf Superconductivity (unpublished).
[12] Alex Gurevich, Maximum screening fields of superconducting multilayer structures, AIP Adv. **5**, 017112 (2015).
[13] Mark W. Coffey and John R. Clem, Unified Theory of Effects of Vortex Pinning and Flux Creep upon the rf Surface Impedance of Type-II Superconductors, Phys. Rev. Lett. **67**, 386 (1991).
[14] Ernst Brandt, Penetration of Magnetic ac Fields into Type-II Superconductors, Phys. Rev. Lett. **67**, 2219 (1991).
[15] C. J. van Der Beek, V. B. Geshkenbein, and V. M. Vinokur, Linear and nonlinear ac response in the superconducting mixed state, Phys. Rev. B **48**, 3393 (1993).
[16] S. Posen, G. Catelani, and M. Liepe, in Proceedings of the Sixteenth Conference on rf Superconductivity, Paris, 2013 (unpublished).
[17] M. Liepe and S. Posen, in Proceedings of the Sixteenth Conference on rf Superconductivity, Paris, 2013 (unpublished).
[18] Nicholas R. A. Valles, Ph.D. thesis, Cornell University, 2014.
[19] D. Saint-James, Angular dependence of the upper critical field of type {II} superconductors; theory, Phys. Lett. **16**, 218 (1965).
[20] H. J. Fink, Vortex nucleation in a superconducting slab near a second-order phase transition and excited states of the sheath near H_{c3}, Phys. Rev. **177**, 732 (1969).

[21] G. Stejic, A. Gurevich, E. Kadyrov, D. Christen, R. Joynt, and D. C. Larbalestier, Effect of geometry on the critical currents of thin films, Phys. Rev. B **49**, 1274 (1994).

[22] V. V. Shmidt, Critical current of an ideal type {II} superconductor in the mixed state, Sov. Phys. JETP **34**, 211 (1972).

[23] Niobium has a fairly low kappa, so the London limit does not apply. In these calculations, the limit used for bulk niobium is when the surface reaches B_{sh} from Table I. For all other materials, the slope of the Gibbs free energy is used as the criterion for flux penetration as described.

[24] T. P. Orlando, E. J. McNiff, S. Foner, and M. R. Beasley, Critical fields, pauli paramagnetic limiting, and material parameters of Nb_3Sn and V_3Si, Phys. Rev. B **19**, 4545 (1979).

[25] Matthias Hein, *High-Temperature-Superconductor Thin Films at Microwave Frequencies* (Springer, New York, 1999).

[26] J. L. Harden and V. Arp, The lower critical field in the Ginzburg-Landau theory of superconductivity, Cryogenics **3**, 105 (1963).

[27] Mark K. Transtrum, Gianluigi Catelani, and James P. Sethna, Superheating field of superconductors within Ginzburg-Landau theory, Phys. Rev. B **83**, 094505 (2011).

[28] B. W. Maxfield and W. L. McLean, Superconducting penetration depth of niobium, Phys. Rev. **139**, A1515 (1965).

[29] M. A. Hein, Markus Perpeet, and Gunter Muller, Nonlinear microwave response of Nb_3Sn films: a case study of granular superconductors, IEEE Trans. Appl. Supercond. **11**, 3434 (2001).

[30] D. E. Oates, Alfredo C. Anderson, C. C. Chin, J. S. Derov, G. Dresselhaus, and M. S. Dresselhaus, Surface-impedance measurements of superconducting NbN films, Phys. Rev. B **43**, 7655 (1991).

[31] Yuxing Wang, Tomasz Plackowski, and Alain Junod, Specific heat in the superconducting and normal state (2–300 K, 0–16 T), and magnetic susceptibility of the 38 K superconductor MgB_2: Evidence for a multicomponent gap, Physica (Amsterdam) **355C**, 179 (2001).

[32] C. P. Bean and J. D. Livingston, Surface Barrier in Type-II Superconductors, Phys. Rev. Lett. **12**, 14 (1964).

[33] G. Catelani and James P. Sethna, Temperature dependence of the superheating field for superconductors in the high-κ London limit, Phys. Rev. B **78**, 224509 (2008).

[34] F. P. Lin and A. Gurevich, Effect of impurities on the superheating field of type-II superconductors, Phys. Rev. B **85**, 054513 (2012).